THE EFFECT OF COMPOSITE BEDS CONTAINING CATALYSTS WITH DIFFERENT ACTIVE METALS ON THE UPGRADING OF A COAL LIQUID

By

ROBERT TALLEY NEWTON, JR.

Bachelor of Science

Oklahoma State University

Stillwater, Oklahoma

1983

Submitted to the Faculty of the Graduate College
of the Oklahoma State University
in partial fulfillment of the requirements
for the Degree of
MASTER OF SCIENCE
December, 1985

THE EFFECT OF COMPOSITE BEDS CONTAINING CATALYSTS WITH DIFFERENT ACTIVE METALS ON THE UPGRADING OF A COAL LIQUID

Thesis Approved:

Billy L Crynes
Thesis Adviser

Mayis Seapan

Harry L Fontah

Norman N. Durham
Dean of the Graduate College

PREFACE

This study was conducted to evaluate the effect of composite beds containing catalysts with different active metals (Ni-Mo, Co-Mo, Ni-W) on the upgrading of a coal liquid. Composite beds containing Ni-Mo catalysts and either Co-Mo or Ni-W catalyts did not have better upgrading performance than beds containing Ni-Mo catalyst in both zones.

I deeply appreciate the help and guidance of my advisor, Dr. Billy L. Crynes. I also appreciate Dr. Mayis Seapan and Dr. Gary L. Foutch for their help. I am grateful to Jirdsak Tscheikuna, Harold Wandke, Ken Dooley, John Beazer, Mark Williams, J. L. Liu, Raul Adarme, Hasan Qabazard, Larry Crynes, Gary Martin, David Tice, and Troy Weiss for their help in operating the equipment. I also want to thank John Carroll, Ann McCollough, Chad Stewart, and Randy Smejkal for their help in analyses. I appreciate Pamela Hartman for her help in typing and editing.

I am grateful for financial support provided by the School of Chemical Engineering and the U.S. Department of Energy (Contract No. DOE/PC 60787).

Finally, I want to express my deep appreciation to my wife, Teena, for her support and inspiration, and my family, for their devotion and encouragement.

TABLE OF CONTENTS

Chapter		Page
I.	INTRODUCTION	1
II.	LITERATURE REVIEW	3
	Upgrading of Alternative Feedstocks	3
	Catalyst Active Metals Effects	4
	Zoned Reactor Beds	6
	Temperature Zones	6
	Pore Sized Zones	7
	Active Metal Zones	9
	Literature Summary	11
III.	EXPERIMENTAL PROCEDURE	13
	Reactor Operation	13
	Reactor System	13
	Preparation	15
	Start Up	15
	Normal Operation	16
	Shutdown	17
	Analyses	17
	Liquid	17
	Catalyst	17
IV.	FEEDSTOCK AND CATALYST PROPERTIES	19
	Feedstock	19
	Catalysts	19
V.	RESULTS AND DISCUSSION	22
	Liquid Analysis	22
	Elemental Analysis	22
	ASTM Distillation	34
	Catalyst Analysis	37
	Coke Content	37
	Support Properties	40
	Metal Deposition	42
	Reactor Operation, Analytical Precision, and Reproducibility	49
	Reactor Operation	49
	Analytical Precision	49
	Reproducibility	50

Chapter Page

VI. CONCLUSIONS AND RECOMMENDATIONS.....56

Conclusions.....56
Recommendations.....57

REFERENCES.....58

APPENDIX.....60

LIST OF TABLES

Table		Page
I.	Feedstock Properties 10 Weight Percent Solids in Process Solvent	20
II.	Catalyst Properties	21
III.	Experimental Conditions for Runs CZA-CZF	23
IV.	Extent of Hydrogenation of Liquid Samples	27
V.	Nitrogen Content of Interstage Samples	29
VI.	Extent of Hydrogenation of Interstage Samples	30
VII.	ASTM Distillation Data of the Feedstock and 60 h Liquid Samples	35
VIII.	Coke Content of Spent Catalysts	38
IX.	Pore Volume and Surface Area of Spent and Regenerated Catalysts	41
X.	Metal Concentrations of the Catalyst Surface	44
XI.	Metal Concentrations at the Catalyst Edge	46
XII.	Metal Concentrations at the Catalyst Middle	47
XIII.	Metal Concentrations at the Catalyst Center	48
XIV.	Hydrogen-to-Carbon Atomic Ratios and ASTM Distillation Data for Runs CZZ and CZF	52
XV.	Catalyst Coke Content for Runs CZA and CZF	54
XVI.	Pore Volume and Surface Area of Spent and Regenerated Catalyst From Runs CZA and CZF	55
XVII.	Nitrogen Content of the Liquid Samples	61
XVIII.	Metal Deposition in Top Zone of Run CZA	62
XIX.	Metal Deposition in Bottom Zone of Run CZA	63

Table Page

XX. Metal Deposition in Top Zone of Run CZB.....64

XXI. Metal Deposition in Bottom Zone of Run CZB.....65

XXII. Metal Deposition in Top Zone of Run CZC.....66

XXIII. Metal Deposition in Bottom Zone of Run CZC.....67

XXIV. Metal Deposition in Top Zone of Run CZD.....68

XXV. Metal Deposition in Bottom Zone of Run CZD.....69

XXVI. Metal Deposition in Top Zone of Run CZE.....70

XXVII. Metal Deposition in Bottom Zone of Run CZE.....71

LIST OF FIGURES

Figure Page

1. Simplified Flow Diagram.....14

2. Effect of Time on Stream on Nitrogen Concentration of Runs CZA, CZB, and CZD.....24

3. Effect of Time on Stream on Nitrogen Concentration of Runs CZA, CZC, and CZE.....25

4. Simplified Process of HDN.....31

5. Qualitative Diagram of the Effect of Catalyst Bed Length on the Concentrations of the HDN Compounds Involved in the Simplified Model of HDN.....32

6. Location of EDAX Scans on the Catalyst Pellets.....43

7. The Effect of Time on Stream on the Nitrogen Concentrations of Runs CZA and CZF.....51

CHAPTER I

INTRODUCTION

As reserves of easily processed petroleum are depleted, other sources of refinery feedstocks will be needed. Since coal constitutes over 75 percent of the recoverable U.S. fossil fuel reserves, coal derived liquids are an attractive alternative.

Several coal liquefaction processes have been developed, including Solvent Refined Coal (SRC), Exxon Donor Solvent (EDS), and H-Coal. However, the products from these processes are unsatisfactory as conventional refinery feedstocks and must be upgraded before use due to large amounts of nitrogen, sulfur, oxygen, and metal containing cyclic compounds. Also, coal liquids are highly aromatic, and therefore, have high molecular weights and are hydrogen deficient. Nitrogen and sulfur concentrations must be reduced to comply with emission regulations, oxygen compounds must be removed to prevent storage difficulties, and metals must be removed to prevent permanent catalyst deactivation due to metals deposition. Coal liquids hydrogen-to-carbon atom ratios must be increased to satisfy fuel standards. Hydrocracking of coal liquids may be necessary to product lighter, more valuable products.

Coal liquids were initially upgraded by processes borrowed from the petroleum industry. These processes, developed primarily for hydrodesulfurization and some hydrodemetallation, are inadequate for coal liquids. New processes have been developed to upgrade feedstocks

containing large amounts of metals, sulfur, and nitrogen. Among these new processes is the concept of zoned reactors.

A zoned reactor is one in which one or more of the process conditions (temperature, pressure, catalyst properties) are varied in two or more zones (stages). These zones may be sections of a single reactor or several reactors in series.

The objective of this study was to investigate the effect of composite bed reactors containing catalysts with different active metals (Ni-Mo, Co-Mo, Ni-W) on the upgrading of an SRC coal liquid. This was accomplished by determining catalyst deactivation for hydrodenitrogenation and hydrogenation, evaluating the amount of coke deposited on the catalysts, loss of catalyst surface area and pore volume, and the recovery of these catalyst properties through regeneration.

CHAPTER II

LITERATURE REVIEW

Upgrading of Alternative Feedstocks

Coal liquids, and other unconventional feedstocks such as petroleum residua and shale oil, are viable alternatives to present petroleum feedstocks. However, effective and economical methods must be developed to upgrade these alternatives for use in conventional refineries.

Alternative feedstocks have been upgraded using techniques developed by the petroleum industry for hydrotreating lighter and cleaner feedstocks. These techniques were usually conducted in isothermal reactors containing a single catalyst and were primarily for hydrodesulfurization (HDS) and hydrodemetallation (HDM). Little hydrodenitrogenation (HDN) activity was evident. However, these techniques were found to be unsuited for upgrading coal liquids, petroleum residues, and shale oils. Rapid catalyst deactivation occurred and interstitial deposits often caused severe reactor plugging. Catalyst deactivation is due to pore blockage caused by coking and metals deposition, and interstitial deposits are usually from metal sulfides (Bhan, 1983). Unconventional feedstocks have such a wide variation of properties that a single catalyst cannot effectively fulfill the process requirements (Nielson et al., 1981). Therefore, zoned reactor processes have been developed to upgrade feedstocks with

high metal and heterocyclic (nitrogen, sulfur, and oxygen containing) content.

The objective of a zoned bed reactor is to improve the performance of processes to upgrade unconventional feedstocks by emphasizing functions such as HDS, HDN, HDM, hydrogenation, and hydrocracking in two or more distinct zones. This zoning is accomplished by varying the process conditions (temperature, pressure, space time) and catalyst properties (average pore diameter, active metals loading, pellet geometry). Individual processes can be tailored to upgrade a specific feedstock. The most common example is the upgrading of a feedstock containing large amounts of metals and sulfur. A composite bed containing an HDM catalyst followed by an HDS catalyst would have less catalyst deactivation and a longer run life than a bed containing only an HDM or HDS catalyst (Miller et al., 1983). Temperatures can be zoned to enhance a specific function. For instance, the temperature in the top zone can be increased to maximize HDS, HDN, and HDM (Arey et al., 1963) or the top zone can be decreased to remove inorganics and heavy residues (Bhan, 1983). Guard beds containing cheap, disposable materials can be used to protect more expensive catalysts downstream (Dooley, 1984).

Catalyst Active Metals Effects

Catalysts that are used for upgrading unconventional feedstocks are usually molybdenum and tungsten, promoted by nickle, cobalt, zinc, and manganese. The most common combinations are Ni-Mo, Co-Mo, Ni-Co-Mo, and Ni-W. Oxides of these metals are usually impregnated on alumina or silica-alumina supports. Support properties typically are 100-325 x 10^3

m^2/kg (0.48-1.59 x 10^6 ft^2/lb) for surface area, 300-600 x 10^{-6} m^3/kg (4.8-9.6 x 10^{-3} ft^3/lb) for pore volume, and 0.5-1.5 x 10^{-6} m (1.6-4.9 x 10^{-6} ft) for average pore diameter (Bhan, 1983).

Mann et al. (1983) studied the effect of alumina supported catalysts containing different metals (Ni-Mo, Co-Mo, Ni-W) on the hydrotreatment of heavy petroleum. Ni-W catalyst was determined to be the best for cracking, hydrogenation and HDS. Ni-Mo catalyst produced the most aromatics and was best for HDN, but worst for HDS. Co-Mo catalyst produced the most paraffins.

Yeh et al. (1984) fabricated sixteen catalysts containing combinations of Ni, Co, Mo, and W on silica-alumina support. Two SRC-II coal liquids, Vacuum Flash Feed (VFF) and Light Ends Column Feed (LECF) were upgraded over the catalysts. Co, Mo, and W enhanced HDN for both feeds but the Co-Mo interaction (effect when both metals are present) decreased HDN. The Co-W interaction also had a negative effect on HDN for the VFF, which had a higher nitrogen content than the LECF. The effect of Co and Mo on HDS of the LECF was positive, but the Co-Mo interaction had a negative effect on the HDS of the LECF. Mo and W had a positive effect on the HDS of the VFF, but Co had a negative effect. The Mo-W interaction had a negative effect on the HDS of the CFF. Ni was found to be ineffectual for the HDS and HDN of both feeds.

Sahin et al. (1984) studied the effect of seven alumina support catalysts containing various concentrations of Ni, Co, Mo, and W on the upgrading of SRC-II LECF. The Ni-Mo combination was the best for HDN and the Co-Mo combination was best for hydrocracking. The Ni-W catalyst was one of the poorest catalysts. Mo was favored over W for the hydrotreatment of this feedstock.

Bhan (1981) investigated the effect of catalysts containing Ni-Mo and Co-Mo on the upgrading of Pamco Process Solvent, an SRC coal liquid. The HDN activity of the Ni-Mo catalyst was greater than the Co-Mo catalyst. Ranganathan et al. (1977) also found Ni-Mo to have a higher HDN effect than Co-Mo at higher temperatures.

Givens et al. (1978) compared the effect of different catalysts on the upgrading of an SRC coal liquid. A Ni-Mo catalyst was more selective and more active for HDN than a Ni-W catalyst. A Co-Mo catalyst was also effective for upgrading coal liquids.

Zoned Reactor Beds

Temperature Zones

Bhan (1983) hydrotreated an SRC coal liquid in a temperature zoned reactor. A small pore, silica-alumina supported, Ni-Mo catalyst was used in both zones. The top zone was operated at 260°C (500°F) and contained 50 percent of the catalyst, while the bottom zone was operated at 400°C (752°F). Nearly all the inorganic and heavy carbonaceous residues were removed in the top zone, and the bottom zone was almost residue free. HDN, hydrogenation, and n-pentane residue removal activities were increased for the temperature zoned reactor over the isothermal reactor, which operated at 400°C (752°F).

Beazer (1984) also hydrotreated an SRC coal liquid in a temperature zoned reactor. Both zones contained a small pore, silica-alumina supported, Ni-Mo catalyst with 20 percent in the top zone. The temperature of the top zone was varied from 400°C (752°F) to 500°C (932°F) while the bottom zone was held constant at 400°C (752°F). Increasing the temperature from 400°C (752°F) to 450°C (842°F)

benefitted HDN and hydrogenation activity. Increasing the temperature from 450°C (842°F) to 500°C (932°F) decreased the catalyst HDN and hydrogenation activity. Coke content and interstitial deposits also increased with temperatures above 450°C (842°F).

Krichko et al. (1984) produced gasoline, diesel fuel, and jet fuel components from brown coal liquefaction products. In order to reduce polymerization, a single pass, two stage process was used. The first stage contained either a Ni-Mo or a Co-Mo commercial catalyst and was operated at 230°C (466°F) to mildly hydrogenate the feedstock. The second stage also contained either a Ni-Mo or a Co-Mo catalyst and was operated at 400°C (752°F) to further hydrogenate and remove nitrogen, sulfur, and phenols from the feed. They used a second two stage process to product jet fuel components from a distillate cut of the coal liquids. The first stage used a noncommercial, wide pore, Ni-Mo catalyst and operated at 380°C (716°F) to hydrogenate and remove nitrogen, sulfur, and phenols from the feed. The second stage contained a sulfided Pd catalyst and operated at 290°C (554°F) to reduce the aromatics content.

Pore Sized Zones

Nielson et al. (1981) presented evidence that optimum reactor performance cannot be obtained with a single catalyst and concluded that composite catalyst beds could lead to better results. Experiments for upgrading heavy petroleum residua were conducted with single bed and multiple bed processes. The single bed unit was used to compare pore size effects in order to design the composite bed. A composite bed was designed containing a wide pore, low activity Mo catalyst in the first

zone, followed by higher activity, Ni-Mo or Co-Mo, catalysts with medium and small pores in the second and third zones, respectively. The sulfur removal activity of the composite bed was 20-65 percent better than for the single catalyst beds.

Bhan (1983) used a composite bed reactor, operated isothermally at 400°C (752°F), to hydrotreat an SRC coal liquid. The reactor contained equal amounts of a small pore catalyst in the top zone and a large pore catalyst in the bottom zone. Both catalysts were silica-alumina supported, Ni-Mo catalysts. The composite bed offerred no significant improvement over single beds with the same catalysts.

Brunn et al. (1975) hydrotreated petroleum residue in two stages. The first stage contained a high HDM catalyst and the second stage contained a coke resistant, high HDS catalyst. Most of the metals deposited in the first stage, which allowed the volume of the second stage to be reduced 50 percent compared to the previous process while still satisfying product specifications. Run life was also extended.

Wolk et al. (1975) reported on a process that employed catalysts of different pore sizes to hydrotreat petroleum residues. The process consisted of a large pore alumina in the top stage for HDM and a small pore Co-Mo catalyst in the bottom stage for HDS. Optimum operation was achieved when the top stage was operated at 415°C (779°F) and the bottom stage was operated at 400°C (752°F).

Miller et al. (1983) compared single catalyst and composite catalyst beds for the hydrotreatment of heavy petroleum. A composite bed containing HDM catalyst in the upper zone and HDS catalyst in the lower zone removed 20 percent more sulfur and 80 percent more metals than a single bed containing only HDS catalyst. At the same sulfur

removal as the single bed, the composite bed allowed the hydrogen pressure to be reduced 30 percent. A composite bed with a larger proportion of HDM catalyst reduced HDS, but greatly extended catalyst life and further reduced hydrogen pressure requirements.

Gibson et al. (1983) discussed development of processes involving graded catalyst hydrotreatment and catalyst pellet geometry for use in a petroleum residuum upgrading unit. A composite bed consisting of an HDM catalyst in the top zone and an HDS catalyst in the bottom zone helped protect the HDS catalyst from deactivation due to metals deposition. Graded catalyst systems had a run life up to 70 percent longer than single catalyst systems. A noncylindrical-shaped catalyst reduced the diffusion effects for HDM and extended the reactor life. A noncylindrical-shaped catalyst could be used in the top zone of a graded catalyst bed to further improve performance.

Frayer et al. (1978) used a graded bed with catalysts of different pellet geometries. The top zone contained a catalyst with alternating longitudinal grooves and protrusions to enhance HDM. The bottom zone contained a cylindrical catalyst pellet for HDS. The graded bed improved the upgrading performance.

Active Metals Zones

Sonnemans et al. (1984) studied new mild hydrocracking (MHC) catalysts for use as second stage catalysts. A multiple bed reactor consisting of a high HDS (Co-Mo) or a high HDN (Ni-Mo) catalyst in the first bed, and a MHC (Ni-Mo) catalyst in the second bed to upgrade heavy petroleum oils. Multiple bed reactors gave better results than single

bed reactors with lighter feeds, and at higher pressures and lower space velocities.

Bhan (1981) compared the performances of composite bed and single bed reactors containing silica-alumina supported Co-Mo and alumina supported Ni-Mo catalysts, in the top and bottom zones, respectively. No improvement of HDN, HDS, or hydrogenation of the SRC coal liquid feedstock was evident.

Fu et al. (1978) conducted a two stage hydroprocessing of an SRC coal liquid. The first stage contained a silica-alumina supported Ni-Mo catalyst and was operated at 415°C (779°F). The second stage contained a silica-alumina supported Ni-W catalyst and was operated at 377°C (711°F) - 433°C (811°F). Hydrogenation, asphaltene reduction, HDN and HDS activity were improved over that of the first stage.

Thompson and Holmes (1985) reported on the hydrotreatment of shale oil in a multistage process. The oil was first hydrotreated in a series of four reactors containing various Ni-Mo catalysts. The oil was then recycled through the first four stages before passing through a series of three reactors containing hydrocracking catalysts. They reported good HDN removal and aromatics reduction.

Aalund (1984) reported on a dual catalyst approach to hydrotreat petroleum vacuum distillates in a mild hydrocracking system. The feedstock was first hydrogenated by an alumina supported Co-Mo catalyst and then hydrocracked by a silica-alumina supported Ni-Mo catalyst. This approach was successful at a commercial refinery. The catalyst was replaced after one year and regenerated for a third catalyst charge to the process.

Guard beds containing cheap, disposable materials have been used to protect more expensive catalysts downstream. Materials such as activated charcoal, alumina, activated clay, glass beads, and used HDS catalysts in a first stage (Dooley, 1984; Johnson et al., 1983) for metal removal, and conventional HDS or HDN catalysts in a second stage have been studied. A reactor can be equipped with two guard beds -- one on stream processing, the other recharging.

Literature Summary

1. Coal liquids, petroleum residua, and shale oil are viable alternatives to present petroleum feedstocks, but must be upgraded prior to direct use in conventional refineries because of high concentrations of nitrogen, sulfur, oxygen and metals, and low hydrogen to carbon ratios.

2. Conventional HDS processes and catalysts developed by the petroleum industry are inadequate for upgrading unconventional feedstocks. New processes and catalysts need to be developed specifically for these feedstocks.

3. Zoned reactors are a promising process for upgrading high metal, high heteroatom, low hydrogen feedstocks since functions such as HDM, HDS, HDN, hydrogenation, and hydrocracking are emphasized.

4. Processes can be individially tailored for specific feedstocks by varying process conditions and catalyst properties.

5. Coal liquid upgrading catalysts are usually Ni-Co, Co-Mo, Ni-Co-Mo, and Ni-W impregnated on alumina or silica-alumina support.

6. Ni-Mo is the best catalyst for HDN and hydrogenation while Co-Mo is the best for HDS and hydrocracking. Ni-W is not as effective as either Ni-Mo or Co-Mo.

7. Catalyst activities and composite bed performance vary greatly for different feedstocks.

8. Temperature zoning can improve performance by influencing hydrotreating functions and hydrocracking.

9. Pore size zoning is an effective process for hydrotreating high metal feedstocks. A large pore catalyst can be used in the top zone to achieve high metals removal while a small pore catalyst can be used in the bottom zone for HDS or HDN.

10. Catalyst pellet geometry can decrease diffusion limitations for HDM and be used in the top zones of composite bed reactors to further improve performance.

11. Composite bed reactors containing catalysts with different active metals can improve HDN, HDS, hydrogenation, and aromatics and asphaltene reduction significantly while extending catalyst life.

12. Guard beds containing cheap, disposable materials can be used to protect more expensive catalysts downstream.

CHAPTER III

EXPERIMENTAL PROCEDURE

The experimental equipment and procedures used in this study were the same used by Bhan (1983). Therefore, only a generalized description is presented here.

Reactor Operation

Reactor System

This study was conducted using a two stage, trickle bed reactor system designed and constructed by Bhan (1983). He and other researchers (Tscheikuna, 1984; Beazer, 1984) operated the system and reported good results. A simplified diagram of the reactor system is presented in Figure 1. The system consisted of two reactors in series in which the feedstock and hydrogen flowed down cocurrently. The top and bottom reactors were 43 cm (17 in) and 46 cm (18 in) long, respectively, and had an inside diameter of 1.1 cm (0.43 in). The reactors were enclosed in aluminum blocks for heat distribution. Constant temperature is maintained with two controllers which regulated the power to electrical heating bands placed around the aluminum blocks. Temperature was measured by thermocouples located in thermewalls inside the reactors and at the external surface of the reactors. A Ruska positive displacement pump delivered the feedstock at a constant rate, and the hydrogen pressure was maintained by a Mity-Mite

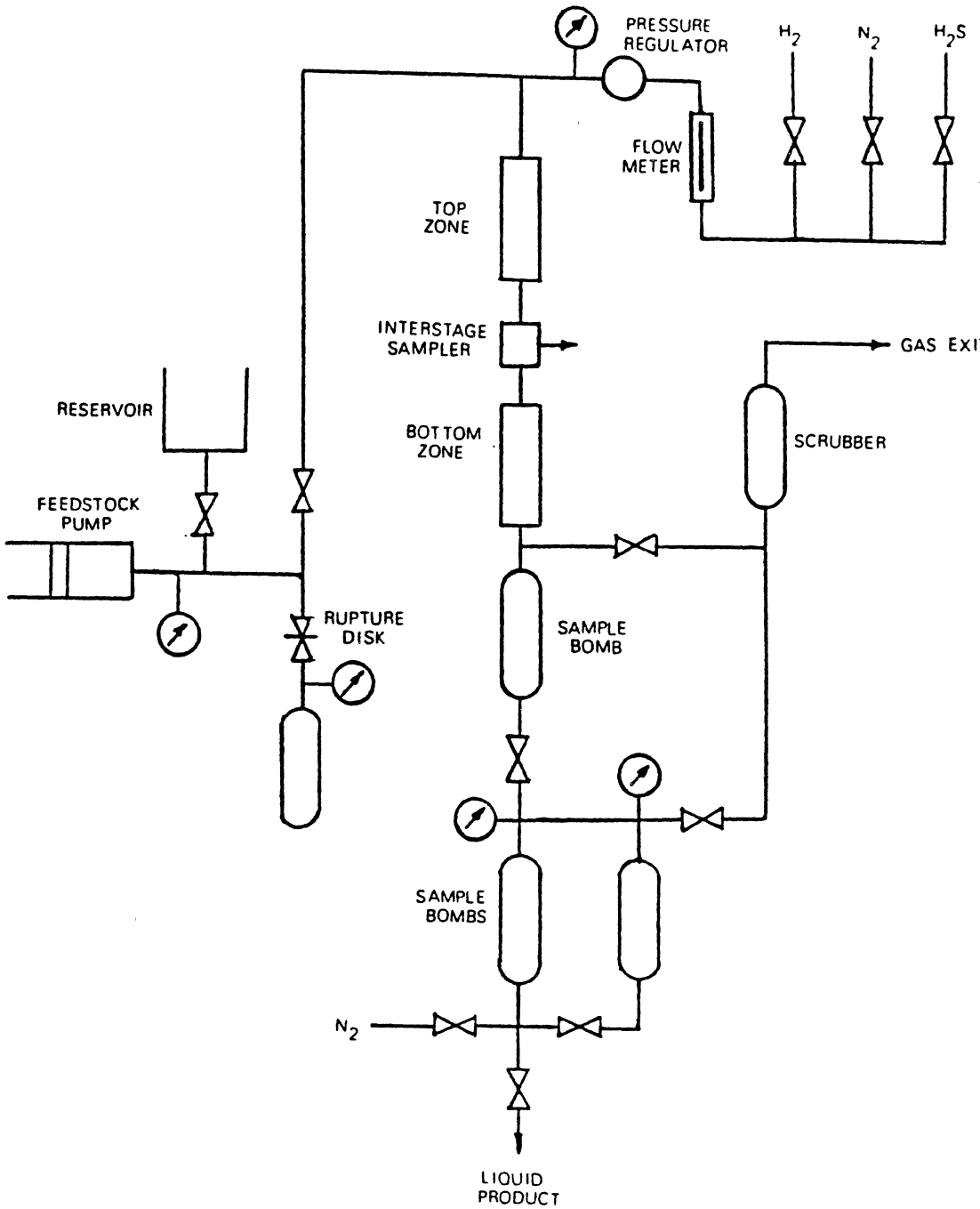

Figure 1. Simplified Flow Diagram

pressure regulator. Hydrogen was delivered from gas cylinders. Rupture disks were located on the feedline to prevent a pressure buildup. The gas exited through one of two lines. The liquid was separated from the gas in the top sample bomb before flowing to the bottom pressure bomb. Liquid samples were collected from the second sample bomb and an interstage sampler located between the reactors. Concentrations of dangerous gases in the laboratory were monitored with hydrogen and hydrogen sulfide detectors.

Preparation

The top and bottom reactors were filled with 15.3 g of catalyst packed to a height of 22.0 cm (8.7 in) and with 10.6 cm (4.2 in) to 11.9 cm (4.7 in) of glass beads before and after the catalysts. The reactor system was then assembled and pressure tested. The system was gradually pressurized with nitrogen and any leaks were sealed. When the system reached the operating pressure, it was closed off for 1.0 h. A pressure drop of 0.13 MPa (20 psi) during this time was considered acceptable.

Start Up

The catalysts were first calcined to remove water and air from the system. Nitrogen was passed through the system at 1.4 MPa (200 psig) and 12 x 10^{-3} m^3/h (424 x 10^{-3} ft^3/h) at standard temperature and pressure, and the temperature was raised to 400°C (752°F) at a rate of 120°C/h (216°F/h). During calcination, the feedstock was heated in a water bath at 90-100°C (176-212°F) and agitated to insure complete mixing. After the catalyst was calcined (4 h), it was sulfided with 30 x 10^{-3} m^3/h (1.06 ft^3/h) of a 5 percent H_2S in H_2 mixture at 400°C

(752°F) and 0.55 MPa (80 psig) for 3 h. During sulfiding, the feedstock was charged to the pump, which along with the feedline were preheated to 100°C (212°F) and 125°C (257°F), respectively. After sulfiding, the system was purged with nitrogen for 0.167 h while the temperature was decreased to approximately 370°C (689°F).

The system was pressurized to 10.3 MPa (1500 psig) with hydrogen, and the flow rate was set at 36 x 10^{-3} m^3/h (1.27 ft^3/h), which corresponds to 1781 m^3 H_2/m^3 feedstock (10,000 ft^3/bbl) at standard temperature and pressure. The pump was raised to the system pressure and turned on at a rate of 20 x 10^{-6} m^3/h (7.0 x 10^{-4} ft^3/h). After the feedstock contacted the catalyst (shown by a temperature rise, about 5-10°C (9-18°F), at the top of th first catalyst zone), the temperature was set at 400°C (752°F).

Normal Operation

The process conditions; 400°F (752°F), 10.3 MPa (1500 psig), 1781 m^3 H_2/m^3 feedstock (10,000 ft^3/bbl) at standard temperature and pressure; were maintained and recorded hourly. Liquid samples were taken every 6 h for the first 48 h, and every 12 h for the remainder of the 72 h schedule.

Liquid samples were taken by redirecting the gas flow to the alternate exit and depressurizing the lower sample bomb. The sample bomb was purged with nitrogen to remove any remaining product gases before the liquid sample was taken.

The interstage sample was taken by closing the system after the first reactor and allowing the liquid to hold up for 0.083 h. The sample was taken and the system returned to normal operation.

Shutdown

After the final samples were taken, the pump and heaters were turned off, but the hydrogen flow was continued until the temperature decreased to about 300°C (572°F). Then nitrogen was passed through the system until the catalysts were at room temperature. Catalyst samples were taken from the top, middle, and bottom sections of each zone.

Analyses

Liquid

Liquid samples were analyzed for nitrogen, carbon, and hydrogen content on a Perkin-Elmer 240B elemental analyzer. Liquid samples taken at the 60 h mark of each run were distilled following ASTM D-1160 at 1.3 x 10^{-3} MPa (0.19 psia). The distillation curves were converted to atmospheric pressure using the ASTM D-2892 conversion tables.

Catalyst

The catalyst samples were Soxhlet extracted with tetrahydrofuran for 24 h to remove any residue, then dried at 200°C (392°F).

Coke content (carbonaceous material) was determined to be the weight percent loss following combustion. The samples were dried under vacuum at 110°C (230°F) for 3 h, cooled and weighed in a helium atmosphere, then baked at 475°C (887°F) for 24 h. The samples were dried and weighed again following the same procedure. Weight loss occurs not only due to the combustion of carbonaceous materials, but also due to the oxidation of active metal sulfides. The data were corrected for the oxidation of the active metal sulfides, but no

correction could be made for the oxidation of the deposited metal sulfides.

Fresh, spent, and regenerated (by combustion) catalyst samples were analyzed for surface area, pore volume, and pore distribution on a Quantochrome Porosimeter. Samples were degassed under a vacuum and put in a helium atmosphere prior to the analysis.

Regenerated catalysts were analyzed for metals by a Scanning Electron Microscope equipped with a JEOL Model JFM-35 Energy Dispersive X-Ray Analysis (EDAX).

CHAPTER IV

FEEDSTOCK AND CATALYSTS PROPERTIES

Feedstock

SRC-I solids and process solvent were obtained from Pittsburg and Midway Coal Mining Company's SRC pilot plant. A mixture of 10 weight percent solids in solvent was prepared. The solution was heated to 125°C (257°F) and agitated for 24 h. Properties of the feedstock are presented in Table I. This feedstock, which has high concentrations of nitrogen and asphaltenes and is hydrogen deficient, was chosen because it is typical of coal liquids. Beazer (1984), Bhan (1983), and Chang (1983) had success upgrading similar SRC feedstocks in a trickle bed reactor.

Catalysts

Three commercial catalysts were used in this study: Armak KF-153S-1.5E (Ni-Mo), Armak KF-124-1.5E (Co-Mo), and Harshaw Ni-4301 E 1/12 (Ni-W). These catalysts were chosen for their similar support properties, geometries, and metal concentrations and because they are representative of commonly used types. The physical properties of the catalysts are given in Table II. The Co-Mo catalyst has the highest surface area, and the Ni-W catalyst has the lowest. Also, the Ni-Mo and Co-Mo catalyst contain silica, which enhances hydrocracking.

TABLE I

FEEDSTOCK PROPERTIES 10 WEIGHT PERCENT
SRC-I SOLIDS IN PROCESS SOLVENT

Elemental Analysis (wt.%)		Boiling Point Curve* Volume Percent	Temperature °C (°F)	
C	88.9	IBP	253	(487)
H	7.9	10	277	(531)
N	1.1	20	293	(560)
S	0.7	30	309	(589)
Ash	0.3	40	327	(621)
O	1.1*			
Density at 20°C (68°F)		50	347	(656)
1.12×10^3 kg·m^{-3}		60	368	(694)
		70	395	(743)
		80	451	(845)
		19.6 wt% 451°C+ (844°F+) residue		

* obtained from ASTM D-1160 and D-2892
**by difference

TABLE II

CATALYST PROPERTIES

	Armak KF-153S	Armak KF-124	Harshaw Ni-4301
Chemical Composition*			
NiO	3.3	---	6.0
CoO	---	4.0	---
MoO_3	15.5	12.0	---
WO_3	---	---	19.0
SiO_2	4.1	1.0	---
Al_2O_3	balance	balance	balance
Physical Properties**			
pellet geometry extrudates (mm)	1.6	1.6	2.1
surface area x 10^3 m^2/kg	302	350	227
pore volume x 10^{-3} m^3/kg	0.488	0.577	0.345
average pore diameter (nm)	6.4	6.4	8.0

* vendor's data
**determined with our analytical equipment

CHAPTER V

RESULTS AND DISCUSSION

Six experimental runs, CZA-CZF, were conducted for this study. The objective of run CZA was to establish reference data with Ni-Mo catalyst in both zones. Runs CZB and CZC were made to evaluate the effect of Co-Mo and Ni-W catalysts, respectively, in the bottom zone, and Ni-Mo catalyst in the top zone. Runs CZD and CZE were made to evaluate the effect of Co-Mo and Ni-W catalysts, respectively, in the top zone, and Ni-Mo catalyst in the bottom zone. Run CZF repeated CZA to determine overall reproducibility. Table III summarizes general information for the runs.

The trickle bed reactor was operated at 400°C (752°F) and 10.3 MPa (1500 psig) with the catalysts divided equally by weight between the two zones. The total (both zones) space time was 1.9 h and the hydrogen flow rate was maintained at 1781 m^3/m^3 feedstock (10,000 SCF/bbl). The flow rate of the feedstock was 20 x 10^{-6} m^3/h (7.0 x 10^{-4} ft^3/h). Analytical precision and reproducibility are discussed following the presentation of the primary results.

Liquid Analysis

Elemental Analysis

Figures 2 and 3 present the nitrogen content of the samples from runs CZA-CZE. The Appendix contains the tabular data. The data show a

TABLE III

EXPERIMENTAL CONDITIONS FOR RUNS CZA-CZF

Run	Upper Zone catalyst (type)	Lower Zone catalyst (type)
CZA	Armak KF-153S (Ni-Mo)	Armak KF-153S (Ni-Mo)
CZB	Armak KF-153S (Ni-Mo)	Armak KF-124 (Co-Mo)
CZC	Armak KF-153S (Ni-Mo)	Harshaw Ni-4301 (Ni-W)
CZD	Armak KF-124 (Co-Mo)	Armak KF-153S (Ni-Mo)
CZE	Harshaw Ni-4301 (Ni-W)	Armak KF-153S (Ni-Mo)
CZF	Armak KF-153S (Ni-Mo)	Armak KF-153S (Ni-Mo)

Temperature - 400°C (752°F)

Pressure - 10.3 MPa (1500 psig)

Total Space Time - 1.9 h (equally divided between zones)

Feedstock - 10 wt% SRC I solids in process solvent

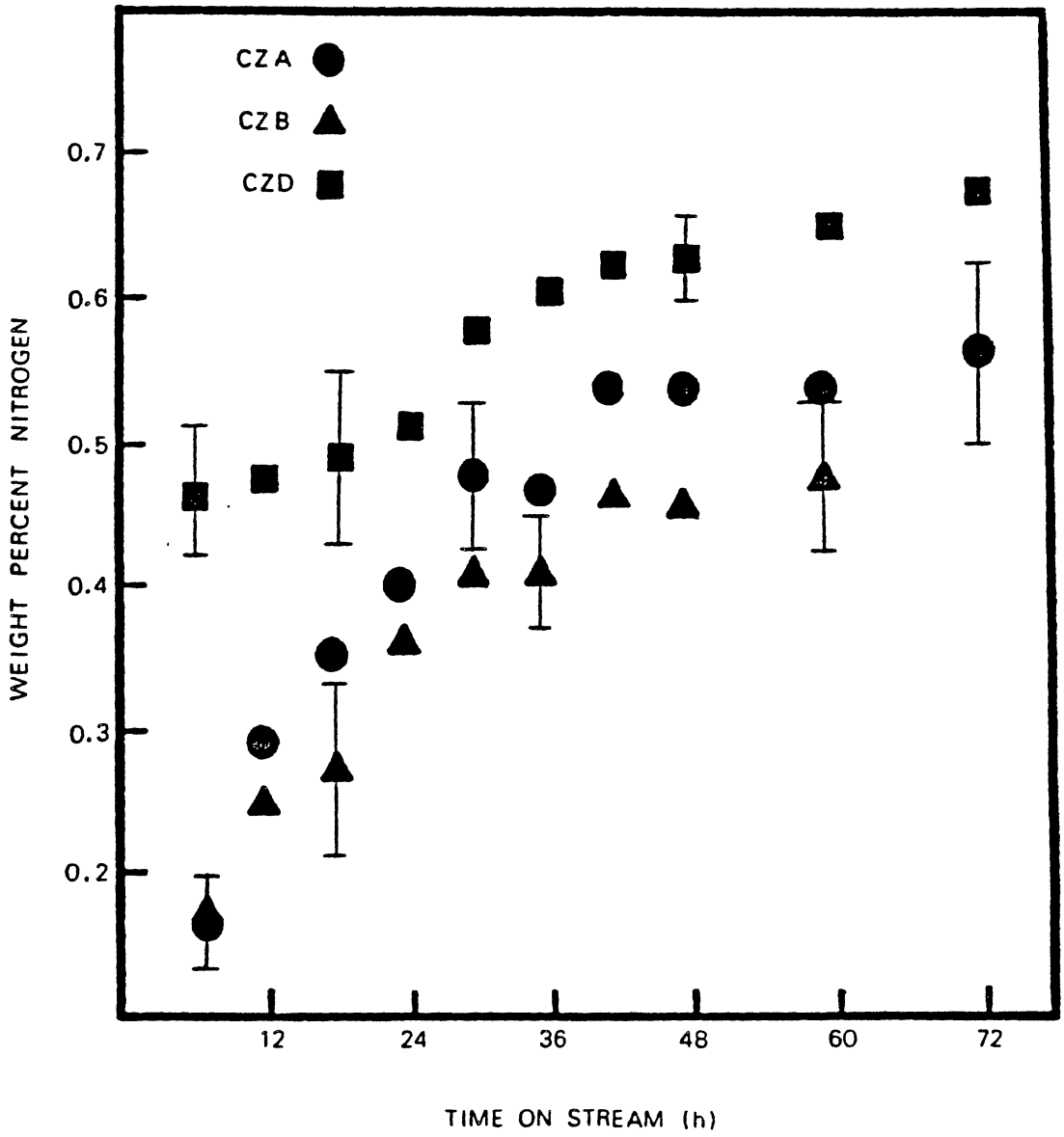

Figure 2. Effect of Time on Stream on Nitrogen Concentration of Runs CZA, CZB, and CZD

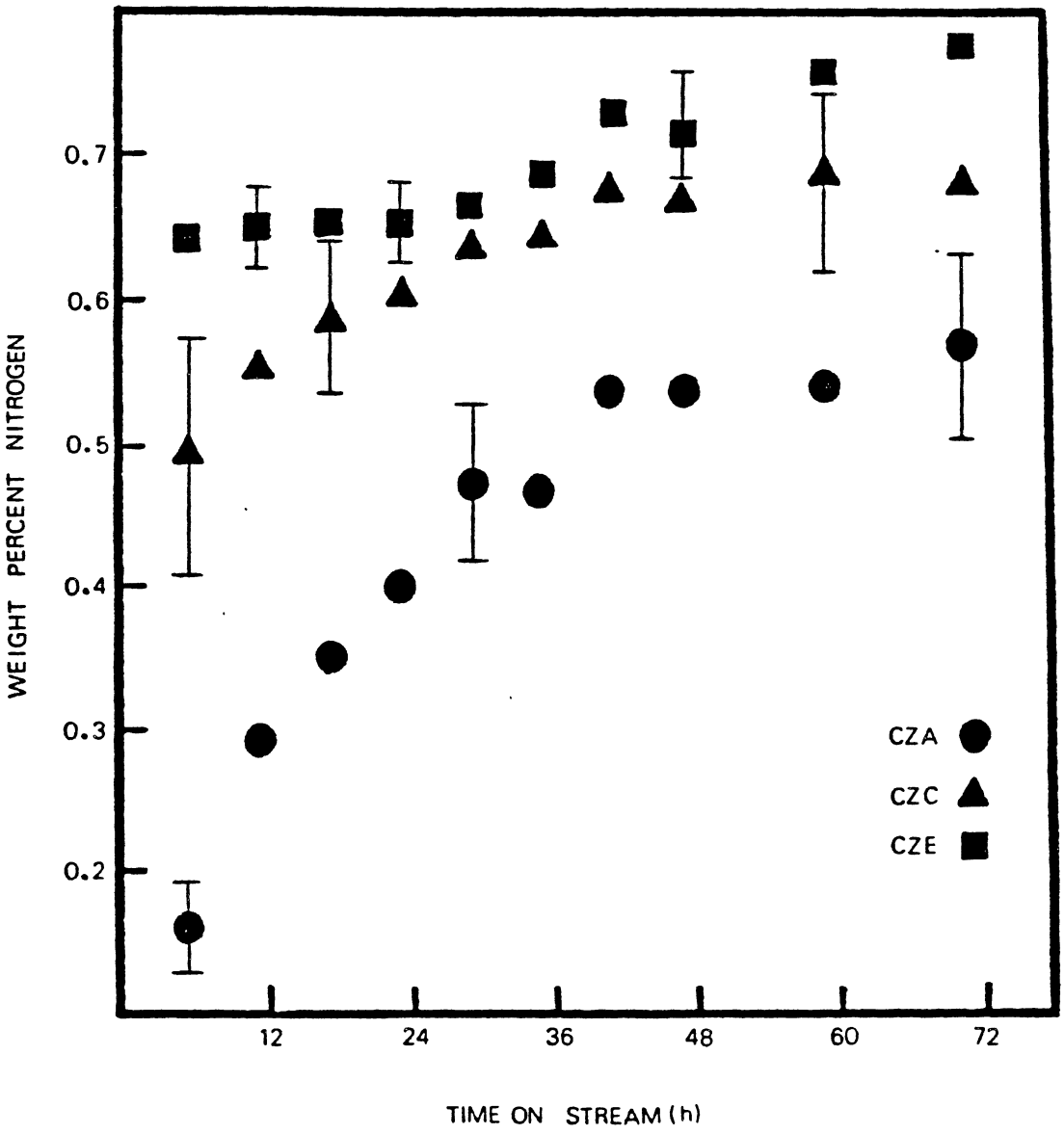

Figure 3. Effect of Time on Stream on Nitrogen Concentrations of Runs CZA, CZC, and CZE

region of rapid catalyst deactivation during the first 24-48 h followed by a region of relatively slow deactivation. Runs CZD and CZE did not have as distinct regions of deactivation as the other runs. Beazer (1984) and Bhan (1983) also reported rapid catalyst deactivation initially followed by slower deactivation while hydrotreating a 15 weight percent SRC solids in process solvent. Chang (1982) also reported this behavior while processing 30 weight percent SRC solids in process solvent. This deactivation can be attributed to rapid coke deposition during the initial period and more gradual coke and metal deposition during the latter period.

The active metal loadings and order of the catalysts influenced the HDN activity significantly. The HDN of runs CZA and CZB were approximately equal and were the best of the runs. These two runs had lower initial nitrogen contents and leveled off at a lower content than runs CZC-CZE. Run CZA contained the Ni-Mo catalysts in both zones and was expected to have very good HDN. Run CZB contained Co-Mo catalyst in the bottom zone, which had a high hydrocracking activity. Run CZD reversed the order of catalysts in run CZB, but had much lower nitrogen removal. Runs CZC and CZE, which both contained Ni-Mo and Ni-W catalysts, but in reversed orders, had the lowest HDN. Run CZC, which had the Ni-Mo catalyst in the top zone, had more HDN than run CZE.

The hydrogenation data are presented as hydrogen-to-carbon (H/C) atomic ratios in Table IV. The data show that the Ni-Mo and Co-Mo catalysts have somewhat higher hydrogenation activities than the Ni-W catalyst. The hydrogenation activity does not have as definite a deactivation trend as the HDN activity did.

TABLE IV

EXTENT OF HYDROGENATION OF LIQUID SAMPLES
(HYDROGEN-TO-CARBON ATOM RATIO)

time on stream (h)	CZA	CZB	CZC	CZD	CZE	CZF
6	1.41	1.29	1.28	1.30	1.41	1.28
12	1.33	1.31	1.34	1.32	1.30	1.31
18	1.29	1.39	1.21	1.30	1.31	1.27
24	1.28	1.23	1.24	1.33	1.28	1.23
30	1.25	1.36	1.22	1.32	1.30	1.29
36	1.27	1.32	1.22	1.30	1.28	1.30
42	1.25	1.29	1.18	1.29	1.25	1.23
48	1.23	1.30	1.21	1.30	1.26	1.31
60	1.25	1.23	1.25	1.36	1.27	1.37
72	1.23	*	1.19	1.29	1.25	1.29
average	1.28	1.30	1.23	1.31	1.29	1.29

Feedstock H/C ratio - 1.07

*Sample not obtained due to early shutdown

The nitrogen contents of the interstage samples are presented in Table V. Runs CZA-CZC contained Ni-Mo catalyst in the top zone and had approximately equal HDN, averaging 0.92 weight percent nitrogen. Run CZD had Co-Mo catalyst in the top zone and had an average nitrogen content of 0.98 weight percent, while Run CZE contained Ni-W catalyst in the top zone and averaged 1.03 weight percent nitrogen. The H/C atomic ratios are given in Table VI. Runs CZA-CZC have the best hydrogenation activity, run CZD is second best, and run CZE is worst. The elemental analyses of the liquid products and interstage samples were consistent with Beazer (1984) and Bhan (1983).

The results from the elemental analysis can be explained using a simplified model of HDN. Nitrogen is predominantly present in coal liquids in polyaromatic compounds. The nitrogen-containing ring must first be saturated with hydrogen, then the nitrogen is severed from the ring and combines with hydrogen to form ammonia. A diagram of this simplified process is given in Figure 4. Since hydrogenation, which is a reversible process, is exothermic, higher temperatures favor dehydrogenation. Beazer (1984) studied temperature zoning effects while upgrading a coal liquid. The top zone was varied 400-500°C (752-932°F) while the bottom zone was held constant at 400°C (752°F). At temperatures above 450°C (842°F), dehydrogenation appeared to be favored. This indicates that hydrogenation-dehydrogenation equilibrium occurs at temperatures near 450°C (842°F).

A qualitative diagram of the effect of bed length on the concentrations of the compounds of the simplified HDN process is given in Figure 5. The amount of nitrogen-containing, unsaturated compounds continually decreases, while the amounts of nitrogen-free compounds and

TABLE V

NITROGEN CONTENT OF INTERSTAGE SAMPLES

	weight percent					
time on stream (h)	CZA	CZB	CZC	CZD	CZE	CZF
6	0.68	0.84	0.74	0.93	1.03	0.74
12	0.84	0.82	0.93	0.96	1.01	0.83
18	0.93	0.84	0.92	0.94	1.04	0.71
24	0.88	0.90	0.97	0.99	0.93	0.96
30	0.92	0.88	0.85	1.01	1.00	0.85
36	0.69	1.08	0.80	1.00	1.11	1.00
42	0.77	0.87	0.99	1.02	1.04	1.08
48	1.08	0.93	0.77	0.96	1.04	0.90
60	1.09	1.06	0.98	1.02	1.04	0.85
72	0.90	*	0.86	0.96	1.08	0.93

feedstock nitrogen content - 1.10 weight percent

*Sample not obtained due to early shutdown

TABLE VI

EXTENT OF HYDROGENATION OF INTERSTAGE SAMPLES
(HYDROGEN-TO-CARBON ATOM RATIOS)

time on stream (h)	CZA	CZB	CZC	CZD	CZE	CZF
6	1.21	1.19	1.18	1.09	1.08	1.17
12	1.25	1.18	1.13	1.08	1.10	1.18
18	1.19	1.19	1.14	1.07	1.09	1.19
24	1.13	1.13	1.17	1.10	1.07	1.12
30	1.09	1.22	1.16	1.07	1.10	1.11
36	1.15	1.16	1.18	1.15	1.08	1.13
42	1.17	1.21	1.17	1.07	1.08	1.19
48	1.15	1.14	1.21	1.11	1.10	1.17
60	1.15	1.14	1.13	1.19	1.09	1.15
72	1.12	*	1.15	1.13	1.07	1.17

feedstock H/C ratio - 1.07

*Sample not obtained due to early shutdown

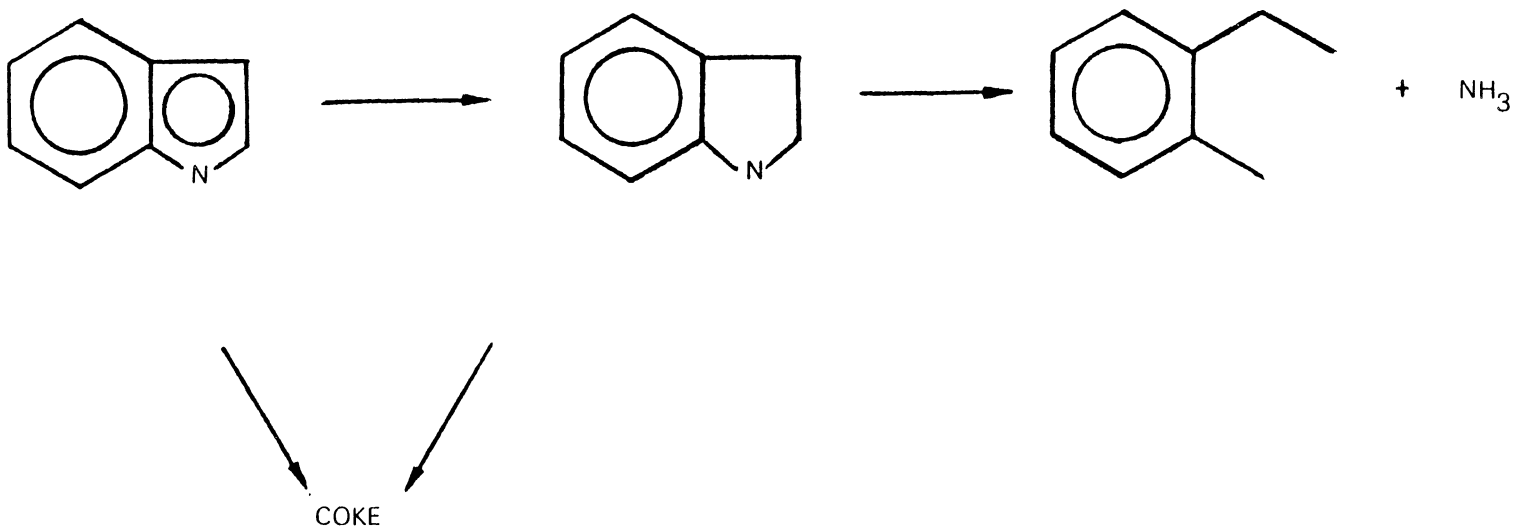

Figure 4. Simplified Process of HDN

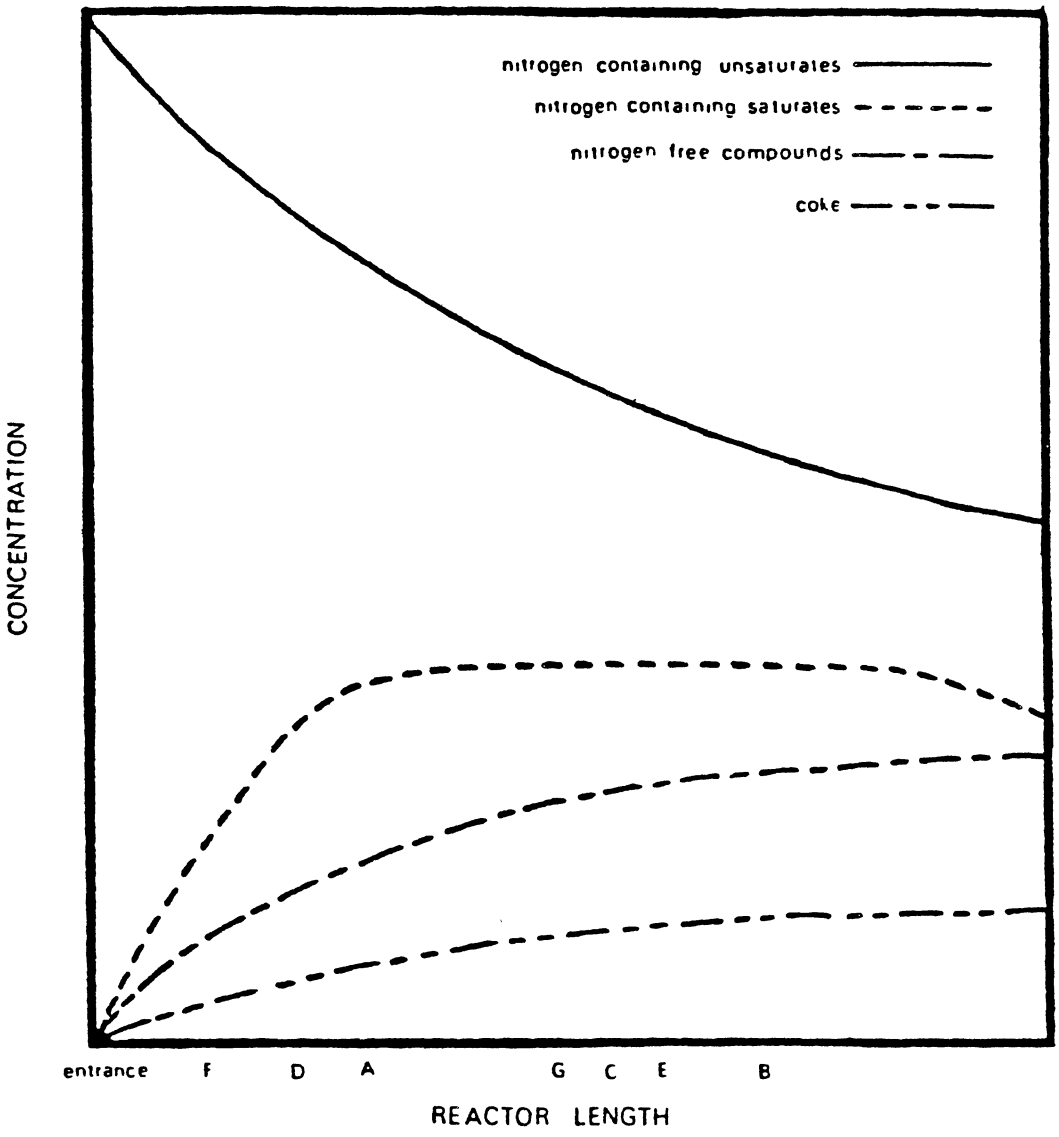

Figure 5. Qualitative Diagram of the Effect of Catalyst Bed Length on the Concentrations of the HDN Compounds Involved in the Simplified Model of HDN

coke steadily increase. The amount of nitrogen-containing, saturated compounds initially rises, levels off due to hydrogenation-dehydrogenation equilibrium, and decreases as the supply of nitrogen-containing, unsaturated compounds diminishes. Though it is difficult to know exactly where the reactor zones occur on the diagram, reasonable estimates can be obtained from the results.

Runs CZA-CZC contained Ni-Mo catalyst in the top zone. The interstage results show that Ni-Mo catalyst has high HDN and hydrogenation activities. This is consistent with other researchers (Sahin, 1984; Ranganathan, 1977). Hydrogenation for runs CZA-CZC probably neared equilibrium, and a high rate of nitrogen removal occurred. The exit of the top zone of runs CZA-CZC was probably near point A on Figure 5. Run CZA continued treating the feedstock with Ni-Mo catalyst, and subsequently, had excellent nitrogen removal. Run CZB contained Co-Mo catalyst in the bottom zone. The interstage results indicate that Co-Mo catalyst is not as good a hydrogenator as Ni-Mo catalyst, but it is an excellent hydrocracker. Hydrogenation equilibrium was probably maintained in the bottom zone while nitrogen-carbon bonds were cracked. The bottom zone for runs CZA and CZB ended near point B. Run CZC contained Ni-W catalyst in the bottom zone, did not remove as much nitrogen as runs CZA and CZB, but hydrogenation was similar. The interstage samples for the Ni-W catalyst removed little nitrogen, which is consistent with research reported by Sahin et al. (1984). The bottom zone for run CZC ended near point C. Run CZD contained Co-Mo catalyst in the top zone and Ni-Mo catalyst in the bottom zone. Some hydrogenation occurred in the top zone, but equilibrium may not have been attained. The interstage samples for run

CZD indicate that some HDN did occur. The end of the top zone was near point D. The bottom zone did reach hydrogenation equilibrium and had good HDN. The bottom zone ended near point E. Run CZE contained Ni-W catalyst in the top zone and little hydrogenation or HDN was evident in the interstage samples. The top zone ended at point F. The Ni-Mo catalyst in the bottom zone reached hydrogenation equilibrium and had good HDN activity. The end of the bottom zone was near point G.

This model, though extremely simplified, helps explain the behavior of the composite beds. Only general shapes and trends of Figure 5 are implied.

ASTM Distillation

Distillation curves for the feedstock and 60 h samples were prepared according to ASTM D-1160 and D-2892 procedures. The data is presented in Table VII. All runs significantly lowered the distillation curve from the feedstock.

The curves for runs containing Ni-Mo or Ni-Mo and Co-Mo (CZA, CZB, CZD) were approximately equal, while the runs containing Ni-Mo and Ni-W (CZC, CZE) were slightly higher. Order of the catalyst had no apparent effect on the distillation curves. The liquid fractions were characterized as light oils - atmospheric boiling point below 216°C (421°F), middle distillate - atmospheric boiling point between 216°C (421°F) and 343°C (649°F), and heavy ends - atmospheric boiling point above 343°C (649°F). The weight percent of the heavy residue not fractionated was recorded. These data are also presented in Table VII.

Light ends were not present in the feedstock, but were present in all liquid samples. The Ni-Mo catalyst run (CZA) produced the most

TABLE VII

ASTM DISTILLATION DATA OF THE FEEDSTOCK AND 60 h LIQUID SAMPLES

Volume Percent	Feed	CZA	CZB	CZC	CZD	CZE
ibp	253	160	191	178	188	204
10	277	253	252	256	247	262
20	293	274	275	277	271	277
30	309	283	288	292	284	293
40	337	295	301	304	297	306
50	347	308	313	319	311	321
60	368	324	328	336	325	332
70	395	343	351	358	352	364
80	451	381	383	390	384	407
light oils T < 216°C (vol %)	0	6	4	3	3	2
middle distillate 216 < T < 343°C (vol %)	48	64	63	60	63	61
heavy ends T > 343°C (vol %)	52	30	33	37	34	37
heavy residue (wt %)	19.6	6.8	8.2	8.9	7.8	9.1

light ends, and the Ni-Mo and Co-Mo containing runs (CZB, CZD) produced the second most. The amount of middle distillate was approximately equal for all runs, but the Ni-Mo and Ni-W containing runs (CZC, CZE) produced the most heavy ends and heavy residue.

The distillation curves are lowered by hydrogenation and hydrocracking of the feedstock. Since hydrogenation for the three catalysts was approximately equal, any differences in the curves were probably due to different hydrocracking activities of the catalysts. The Ni-Mo and Co-Mo catalysts had higher hydrocracking activities. Hydrocracking is enhanced when either Co or silica is present. Both the Ni-Mo and Co-Mo catalysts contained silica (4.1 and 1.0 weight percent, respectively), which caused higher hydrocracking activity than the Ni-W catalyst, which had no Co or silica present. The additional silica in the Ni-Mo catalyst probably compensated for the Co present in the Co-Mo catalyst.

The liquid analysis can be summarized as follows:

1. In all runs, rapid catalyst deactivation occurred during the first 24-48 h. The deactivation rate leveled off for the remainder of the run.
2. Composite beds containing catalysts with different metal loading (Ni-Mo, Co-Mo, Ni-W) did not improve hydrotreatment compared to single beds containing the best catalyst (Ni-Mo).
3. Ni-Mo catalyst was the best for hydrogenation and HDN. Ni-Mo and Co-Mo catalyst were approximately equal for hydrocracking. Ni-W catalyst was the poorest for hydrogenation, HDN, and hydrocracking.

Catalyst Analysis

Both catalyst zones were divided into upper, middle, and lower sections. The spent catalysts were extracted with tetrahydrofuran and dried. The catalysts were then analyzed for surface area and pore volume. Coking was determined by the catalyst weight loss due to combustion. The regenerated (by combustion) catalysts were analyzed for surface area and pore volume. Metal deposits were identified and located with a scanning electron microscope equipped with a JEOL Model JFM-35 Energy Dispersive X-Ray Analysis (EDAX).

Coke Content

The catalyst weight loss due to combustion at 475 ± 25°C (887 ± 45°F) was calculated. However, not all weight loss was due to the combustion of carbonaceous materials. Both active metal loadings and metal deposits are present in sulfides. Oxidation of these sulfides results in weight loss. Since the concentration of metal sulfides was known, a correction for the weight loss was calculated, but since the concentration of the metal deposits could not be determined, no correction was made for these sulfides.

The data (Table VIII) range from 20-27 weight percent coke (based on fresh catalyst). The top zones tended to contain more (0-3.8 weight percent) coke than the bottom zones, but the profiles for each zone were relatively level. This indicates that coking equilibrium had been attained (Chang, 1982). The coke contents for the six catalysts were approximately equal. The average coke content for the three runs were 24.1, 22.0. and 22.2 weight percent for the Ni-Mo, Co-Mo, and Ni-W catalysts, respectively.

TABLE VIII

COKE CONTENT OF SPENT CATALYSTS

	weight percent				
Top Zone	CZA	CZB	CZC	CZD	CZE
Upper	26.4	25.9	26.0	21.7	27.0
Middle	24.9	27.3	24.7	21.8	18.8
Lower	24.8	25.0	23.9	22.4	24.2
Average	25.4	26.1	24.9	22.0	23.3
Bottom Zone					
Upper	25.9	24.1	21.2	21.7	23.9
Middle	20.1	22.23	21.9	21.8	22.5
Lower	22.8	20.7	20.1	20.6	22.6
Average	22.9	22.4	21.1	21.4	23.0

The amount of coking is affected by feedstock characteristics, reactor conditions, and catalyst type (active metal loadings and support properties). The feedstock and condition for all runs were the same so any differences in the coke content were due to catalyst differences.

Large pore catalysts and hydrocracking catalysts have higher coke contents than small pore catalysts and hydrotreating catalysts. Catalysts with large pores are more accessable for large, polyaromatic molecules that are strong coke precursors. Bhan (1983) upgraded an SRC coal liquid over commercial, large pore and small pore catalysts and found that the large pore catalyst had substantially more coking than the small pore catalyst. Catalysts that have high hydrocracking activities relative to hydrogenation activities also have higher coke contents. During the upgrading of a coal liquid, compounds are cracked and either hydrogenate or combine with other cracked compounds to form coke. Therefore, if the hydrogenation activity is too low relative to the hydrocracking activity, more coke will be formed.

The coke contents for the three catalysts were approximately equal, even though the active metal loadings and support properties were different. The Ni-W had the largest pore diameter and the Co-Mo and Ni-Mo catalyst had the smallest. The Ni-W catalyst, therefore had a higher coke content due to its support properties. The Ni-Mo and Co-Mo catalysts, however, had higher hydrocracking activities than the Ni-W catalyst due to the presence of Co and silica. The Ni-Mo and Co-Mo catalyst, then had higher coke contents due to their active metal loadings. The effect of the pore diameter of the Ni-W catalyst and the hydrocracking activities of the Ni-Mo and Co-Mo catalysts effectively balanced coke contents.

Support Properties

Spent and regenerated catalysts were analyzed for surface area and pore volume. The data are presented in Table IX. Substantial losses in both surface area and pore volume occurred for all spent catalysts, but excellent recovery of these properties was achieved through regeneration. No effect of composite beds on the loss of support properties was evident.

The surface area and pore volume of the spent catalysts was proportional to the distance from the reactor entrance. At the entrance of the top zone, surface area and pore volume losses were the greatest, and the farther into the reactor, the less severe the losses were. Losses in surface area and pore volume are due to coke and metal deposition. Since the coke content was relatively constant in each zone, additional losses were probably due to metal deposition. The metal deposition was greatest at the entrance of the reactor, and decreased through the length of the reactor. This is consistent with Gibson and Green (1983), who reported that metals tend to deposit in the top sections of catalysts beds.

The average pore volume losses were similar for the Ni-Mo, Co-Mo, and Ni-W catalysts (53, 57, and 55 percent, respectively) but the average surface area losses varied significantly (38, 45, and 70 percent, respectively). Recovery of pore volume and surface area through regeneration was over 93 percent for the Ni-Mo and Co-Mo catalysts, but only 85 percent for both the original pore volume and surface area of the Ni-W catalyst was recovered.

The Ni-W catalyst lost more surface area, and recovered less pore volume and surface area through regeneration, than the Ni-Mo and Co-Mo

TABLE IX

PORE VOLUME AND SURFACE AREA OF SPENT AND REGENERATED CATALYSTS

Pore Volume (x 10^{-9} m^3/kg)
Spent/Regenerated

Top Zone	CZA	CZB	CZC	CZD	CZE
Upper	0.152/1.424	0.128/0.456	0.112/0.417	0.167/0.511	0.169/0.307
Middle	0.244/0.431	0.143/0.432	0.185/0.416	0.190/0.539	0.162/0.320
Lower	0.279/0.455	0.128/0.480	0.256/0.488	0.243/0.568	0.151/0.326
Bottom Zone					
Upper	0.226/0.424	0.204/0.577	0.126/0.345	0.220/0.432	0.251/0.464
Middle	0.318/0.448	0.299/0.577	0.159/0.345	0.267/0.480	0.304/0.472
Lower	0.318/0.472	0.374/0.539	0.171/0.316	0.272/0.881	0.346/0.472

Surface Area (x 10^3 m^2/kg)
Spent/Regenerated

Top Zone	CZA	CZB	CZC	CZD	CZE
Upper	122/289	109/287	99/271	117/312	60/147
Middle	193/283	122/291	153/260	155/333	71/173
Lower	218/302	183/298	212/298	206/331	73/207
Bottom Zone					
Upper	191/274	171/312	52/200	170/271	203/294
Middle	232/285	229/336	74/215	200/298	240/291
Lower	234/287	286/350	85/218	217/293	250/293

catalysts. Since the coke contents of the three catalysts were approximately equal, the additional losses in the Ni-W catalyst were probably due to metal deposition. The Ni-W catalyst had a larger pore diameter (8.0×10^{-9} m) than the Ni-Mo and Co-Mo catalysts (6.4×10^{-9} m, each). This is consistent with Nielson et al. (1981), who reported that large pore catalysts had larger metal uptake capacities than small pore catalysts.

Metal Deposition

An electron scanning microscope equipped for EDAX analysis was used to determine the indentity, location, and semi-quantitative concentrations of metal concentrations on the catalysts. The concentrations are based on area percent, and comparisons are valid only for like metals i.e. Fe concentrations can only be compared to Fe concentrations, Zn or Ti concentrations. The surface of the catalyst pellet was scanned once, and the cross section (radial fracture) was scanned three times (Figure 6).

The Fe, Cu, and Ti concentrations deposited on the catalyst surface are listed in Table X. A relatively low concentration of Al (Appendix) indicated an inorganic crust with a high metal concentration covered the catalyst pellets. The crust tended to be thicker at the entrance of each catalyst zone. The average Al concentration of the Ni-W catalyst (5.7 percent) was much lower than the Ni-Mo (33 percent) or the Co-Mo (31 percent) catalysts, indicating a thicker crust on the Ni-W catalyst. Beazer (1984) and Bhan (1983) also reported the formation of an inorganic crust while upgrading an SRC coal liquid. These results support the pore volume and surface area data which indicated that metal

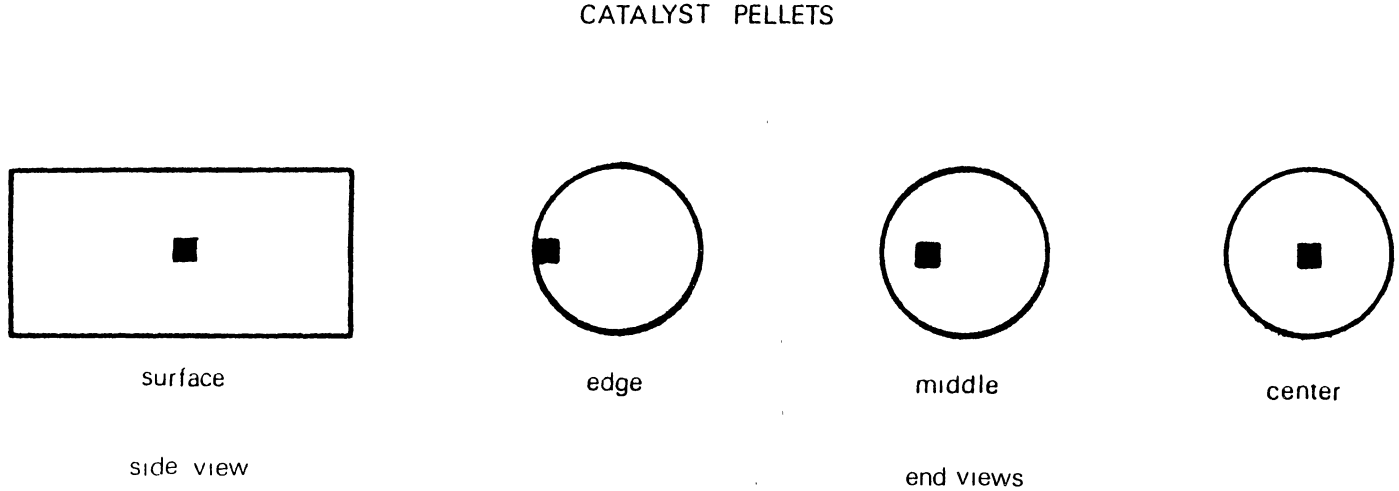

Figure 6. Location of EDAX Scans on the Catalyst Pellets

TABLE X

METAL CONCENTRATIONS ON THE CATALYST SURFACE

Run	Zone	area percent Fe	Cu	Ti
CZA	top	15.4	2.8	3.9
	bottom	13.3	3.4	7.7
CZB	top	23.9	3.4	3.5
	bottom	16.0	15.4	1.9
CZC	top	28.0	3.5	2.3
	bottom	21.7	8.7	1.6
CZD	top	12.3	6.5	9.9
	bottom			
CZE	top	21.1	2.1	-
	bottom	8.0	3.6	5.9

deposits concentrate at the entrance of reactors and that the Ni-W catalyst has more metal deposits than the Ni-Mo or Co-Mo catalysts.

Cross sections of the catalysts were scanned for metal content at the center, middle, and edge. Fe, Cu, and Ti concentrations of the cross sections are listed in Tables XI, XII, and XIII. The metal concentrations were highest at the edge and lowest at the center. The Al concentrations (Appendix) also indeicated more metals deposited at the edge.

The catalyst analysis can be summarized as follows:

1. Coke content were approximately equal for the three catalysts due to the high hydrocracking activity of the Ni-Mo and Co-Mo catalysts and large pore diameter of the Ni-W catalyst.
2. All spent catalysts had severe pore volume and surface area reductions, but these properties were recovered through regeneration to above 93 percent for the Ni-Mo and Co-Mo catalysts and above 85 percent for the Ni-W catalysts.
3. Metal deposits were more concentrated at the entrance of the reactor.
4. The Ni-W catalyst contained more metal deposits due to its larger pore diameters.
5. The effect of catalyst zoning on metal deposition could not be accurately determined since the EDAX analysis is only semi-quantitative.

TABLE XI

METAL CONCENTRATIONS AT THE CATALYST EDGE

Run	Zone	area percent Fe	Cu	Zn
CZA	top	4.2	3.9	1.3
	bottom	14.2	29.1	7.9
CZB	top	10.8	15.9	5.9
	bottom	12.2	13.4	5.0
CZC	top	16.1	12.3	3.9
	bottom	22.8	18.6	2.2
CZD	top	15.9	17.4	5.3
	bottom	20.5	21.3	5.6
CZE	top	4.5	8.6	0
	bottom	9.1	10.8	2.8

TABLE XII

METAL CONCENTRATIONS AT THE CATALYST MIDDLE

Run	Zone	area percent Fe	Cu	Zn
CZA	top	3.7	3.6	1.1
	bottom	13.3	18.0	5.7
CZB	top	10.0	13.3	4.6
	bottom	7.9	12.2	3.8
CZC	top	8.1	8.1	2.4
	bottom	8.8	7.3	0
CZD	top	5.0	15.3	4.0
	bottom	3.7	3.2	0.3
CZE	top	18.5	15.4	0
	bottom	14.4	17.7	5.5

TABLE XIII

METAL CONCENTATIONS AT THE CATALYST CENTER

Run	Zone	area percent Fe	Cu	Zn
CZA	top	3.4	3.3	0.9
	bottom	5.4	7.7	2.9
CZB	top	11.4	17.0	6.7
	bottom	9.7	14.0	4.4
CZC	top	6.4	9.0	3.2
	bottom	6.5	5.0	0
CZD	top	13.4	13.7	3.7
	bottom	4.8	4.6	1.0
CZE	top	12.0	9.8	0
	bottom	5.9	8.3	2.5

Reactor Operation, Analytical Precision, and Reproducibility

Reactor Operation

The reactor conditions were maintained at 400°C (752°F), 10.3 MPa (1500 psig), 20 x 10^{-6} m^3/h (7.0 x 10^{-4} ft^3/h) feedstock, and 1781 m^3H_2/m^3 feedstock (10,000 SCF/bbl).

Isothermal operation was required. The temperature in each zone was maintained by a separate controller. The standard deviations of the top and bottom zones were ± 3.9°C (± 7.0°F) and ± 2.6°C (± 4.7°F), respectively. The deviation was caused by the top section of each zone having a slightly higher temperature than the middle and lower sections, and should not have affected the data.

Pressure was very constant with a standard deviation of ± 51 x 10^{-3} MPa (7.5 psi). Deviations were caused by slight reactor plugging. A positive displacement pump delivered the feedstock. Negligible flucuations occurred during the 72 h run. The hydrogen flow (occasionally) fluctuated between 900-3600 m^3/m^3 feedstock (5000-20,000 SCF/bbl), but since excess hydrogen was provided even at 270 m^3H_2/m^3 feedstock (1500 SCF/bbl) according the Sooter (1975), Satchell (1974), and Wan (1974), the fluctuations should not have affected the data.

Analytical Precision

Liquid samples were analyzed for nitrogen, carbon, and hydrogen content twice in order (6-72 h) and twice in reverse order (72-6 h) to negate any time effects the analyzer had. Concentrations of nitrogen were 0.08-1.1 weight percent with standard deviations of ± 0.01-± 0.19

weight percent. The H/C atomic ratios were 1.18-1.41 with standard deviations of ± 0.02 to ± 0.07.

The products were only distilled once due to the limited sample amounts, but the feedstock was distilled three times. The temperature did not vary more than 3°C (5.4°F), while ASTM requirements are a maximum of 4.4°C (8°F).

The coke contents were 20-27 weight percent (based on fresh catalyst weight). The catalyst sample from the middle section of the bottom zone of run CZF was analyzed three times for an average coke content of 23.1 weight percent and a standard deviation of ± 1.2 weight percent.

Spent and regenerated catalysts were analyzed for pore volume and surface area. Spent catalysts pore volumes and surface areas were 0.151-0.577 x 10^{-3} m^3/kg and 52-355 x 10^3 m^2/kg. Fresh catalysts were analyzed three times each. The pore volumes and surface areas for the Ni-Mo, Co-Mo, and Ni-W catalysts were 0.488 ± 0.024, 0.577 ± 0.031, and 0.345 ± 0.007 x 10^{-3} m^3/kg, respectively, and 302 ± 14.2, 350 ± 4.4, and 227 ± 2.5 x 10^3 m^2/kg, respectively.

Reproducibility

Run CZF duplicated CZA (Ni-Mo catalyst in both zones) in an attempt to determine reproducibility. The nitrogen content of both runs is compared in Figure 7. H/C atomic ratios and ASTM distillation curves are presented in Table XIV. The data show good agreement and are within experimental error. Any deviations were probably caused by irregular flow in the catalyst bed.

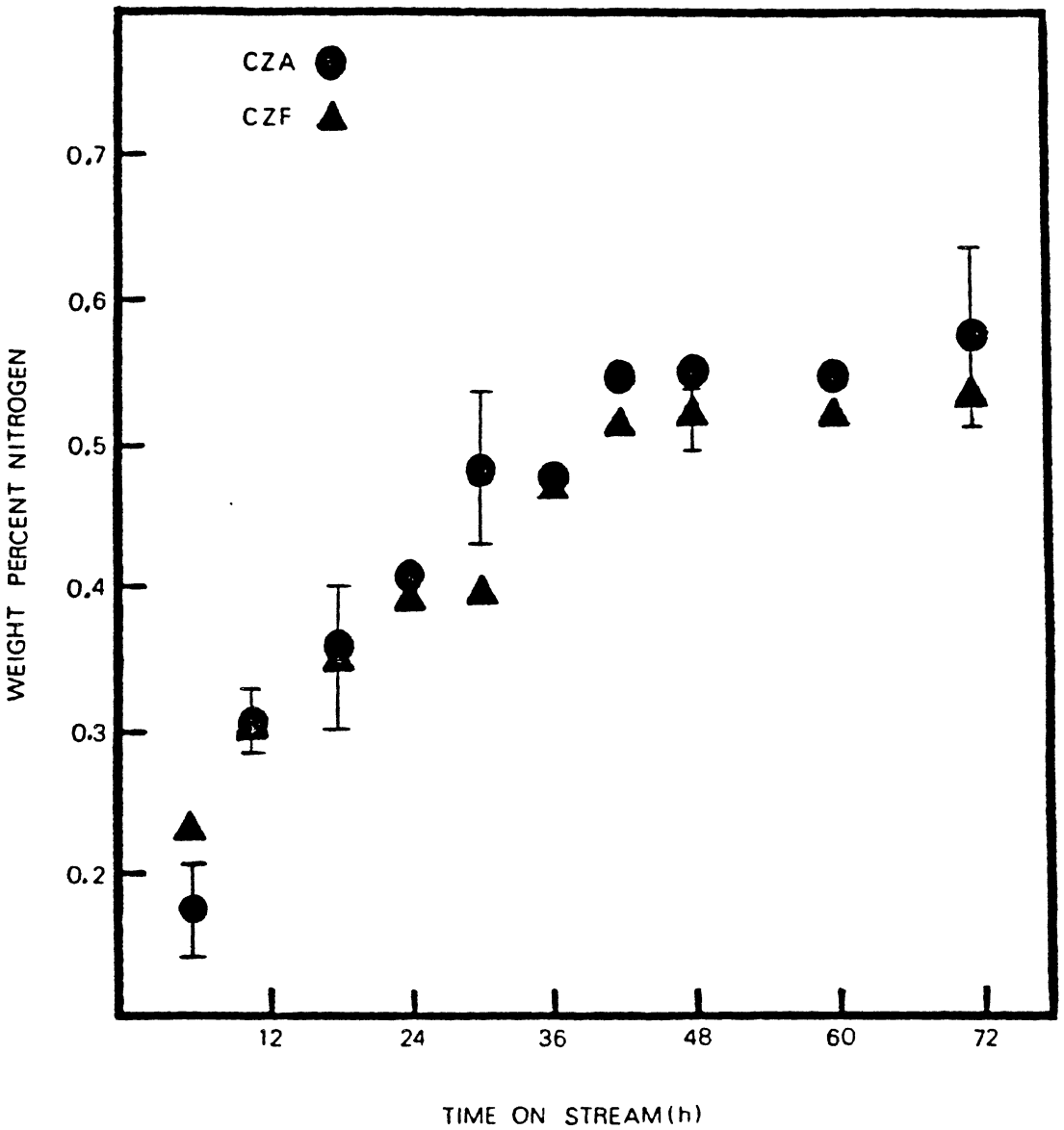

Figure 7. The Effect of Time on Stream on the Nitrogen Concentration of Runs CZA and CZF

TABLE XIV

HYDROGEN-TO-CARBON ATOMIC RATIOS AND ASTM DISTILLATION DATA FOR RUNS CZA AND CZF

H/C Ratio			ASTM Distillation T (°C)		
time on stream (h)	H/C CZA	CZF	volume percent	CZA	CZF
6	1.41	1.28	ibp	160	155
12	1.33	1.31	10	253	249
18	1.29	1.27	20	274	272
24	1.28	1.23	30	283	280
30	1.25	1.29	40	295	293
36	1.27	1.30	50	308	307
42	1.25	1.23	60	324	324
48	1.23	1.31	70	343	345
60	1.25	1.37	80	381	376
72	1.23	1.29	90	464	464
average	1.28	1.29	residue (wt%)	6.8	6.9

Table XV compares the catalyst coke content. The average coke contents of runs CZA and CZF are 25.4 and 25.6 weight percent, respectively, in the top zone, and 23.0 and 22.9 weight percent, respectively, in the bottom zones. The standard deviations for the top and bottom zones are ± .014 and ± 0.05 weight percent, respectively.

Pore volume and surface area data of spent catalysts are given in Table XVI. The average values for the pore volumes and surface areas of the top zones of runs CZA and CZF were 0.225 and 0.206 x 10^{-3} m^3/kg, respectively, and 178 and 175 x 10^3 m^2/kg, respectively. The standard deviations for the pore volume and surface areas in the top zone were 0.013 x 10^{-3} m^3/kg and 2.12 x 10^3 m^2/kg. The average values for the pore volumes and surface areas of the bottom zones of runs CZA and CZF were 0.287 and 0.299 x 10^{-3} m^3/kg, respectively, and 319 and 327 x 10^3 m^2/kg, respectively. The standard deviations for the pore volume and surface area were 0.008 x 10^{-3} m^3/kg and 5.19 x 10^3 m^2/kg.

The deviations presented are consistent with values reported by Beazer (1984) and Bhan (1983). The small deviations and good agreement for HDN, hydrogenation, ASTM distillations, catalyst coke content, and catalyst surface area and pore volumes indicate that the results are precise and reproducible.

TABLE XV

CATALYST COKE CONTENT FOR RUNS CZA AND CZF

	weight percent	
	CZA	CZF
Top Zone		
Upper	26.4	24.2
Middle	24.9	25.5
Lower	24.8	27.0
Average	25.4	25.6
Bottom Zone		
Upper	25.9	24.4
Middle	20.1	23.1
Lower	22.8	21.1
Average	22.9	22.9

TABLE XVI

PORE VOLUME AND SURFACE AREA OF SPENT AND REGENERATED CATALYST FROM RUNS CZA AND CZF

	Pore Volume ($\times 10^{-3}$ m^3/kg) spent/regenerated		Surface Area ($\times 10^3$ m^2/kg) spent/regenerated	
Top Zone	CZA	CZF	CZA	CZF
upper	0.152/0.424	0.175/0.368	122/289	149/257
middle	0.244/0.431	0.205/0.456	193/283	177/283
lower	0.279/0.455	0.239/0.448	218/302	200/285
Bottom Zone				
upper	0.226/0.424	0.240/0.456	191/274	193/293
middle	0.318/0.448	0.300/0.464	232/285	240/288
lower	0.318/0.472	0.357/0.472	234/287	278/284

CHAPTER VI

CONCLUSIONS AND RECOMMENDATIONS

Conclusions

A two-stage, trickle bed reactor was successfully used to upgrade a coal liquid in composite beds containing catalyst with different active metal loadings. The following conclusions can be drawn from this study.

1. This work demonstrated that composite beds did affect upgrading performance (HDN hydrogenation, hydrocracking). However, the composite beds did improve performance over beds containing the best catalyst (Ni-Mo) in both zones. A composite bed contaiing Ni-Mo catalyst in the top zone and Co-Mo catalyst in the bottom zone did perform as well as the bed containing Ni-Mo catalyst in both zones.

2. Composite beds containing the best hydrogenation and HDN catalyst (Ni-Mo) in the top zone and Co-Mo or Ni-W catalysts in the bottom zone had better nitrogen removal than beds containing the same catalysts in reverse order.

3. The Ni-Mo catalyst had the highest hydrogenation and HDN activities and the Co-Mo had the second highest. The Ni-Mo and Co-Mo had approximately equal hydrocracking activities. The Ni-W was the poorest catalyst for this feedstock at these conditions.

4. All runs had a period of rapid catalyst deactivation during the first 24-48 h followed by a period of relatively slow deactivation. Deactivation was attributed to coke and metal deposition.

5. The coke content of the top zone was slightly higher than that of the bottom zone. Coke contents were approximately equal for the three catalysts.

6. The concentration of the metal deposits was highest at the entrance of the reactor and decreased through the length. The Ni-W catalyst contained more metal deposits than the Ni-Mo and Co-Mo catalysts.

7. Pore volume and surface area losses for the spent catalysts were significant, but regeneration by combustion improved these properties to at least 85 percent of the original values.

Recommendations

1. This study showed that both catalyst active metal and support properties affected upgrading perfrmance. Composite beds containing catalysts with both active metal loading and support properties differences should be investigated.

2. This study distributed the catalysts evenly between both zones. The effect of varying catalysts distributions between zones on upgrading performance should be investigated.

3. Rapid catalyst deactivation occurred during the initial period of each run. The effect of low temperature during startup on the initial period of catalyst deactivation should be investigated.

REFERENCES

Aalund, L. R.; Oil and Gas Journal, November 26, 82 (1984).

Arey, W. F., R. B. Mason, D. Springs, and R. C. Paule; U. S. Patent No. 3,254,017; May 31 (1963).

Beazer, J. R.; M.S. Thesis, Oklahoma State University, Stillwater, Oklahoma (1984).

Bhan, O. K.; M.S. Thesis, Oklahoma State University, Stillwater, Oklahoma (1981).

Bhan, O. K.; Ph.D. Dissertation, Oklahoma State University, Stillwater, Oklahoma (1983).

Brunn, L. W., A. A. Montagra, and J. A. Paraskos, Progress in Processing Synthetic Crudes and Resids, Div. of Pet. Chem.; ACS, Chicago Meeting, August 24-29 (1975).

Chang, H.; Ph.D. Dissertation, Oklahoma State University, Stillwater, Oklahoma (1982).

Dooley, K. A.; M.S. Thesis, Oklahoma State University, Stillwater, Oklahoma (1984).

Frayer, J., H. Lese, J. McKinney, K. Metzer, J. Paraskos; U. S. Patent No. 4,118,310, October 3 (1978).

Fu, Y. C., B. F. Rand, J. C. Winslow; Preprints Div. of Fuel Chem., 23, 1, 81 (1978).

Gibson, K. R. and D. C. Green; CEP, May 93 (1983).

Givens, E. N., M. A. Collura, R. W. Skinner, and E. J. Greskovichy; Hydrocarbon Processing, 57, 3, 195 (1978).

Johnson, C.; U. S. Patent No. 4,409,092, October 11 (1983).

Krichko, A., M. Yulin, A. Maloletrev, Y. Petrov; Khim, Tekhnol. Topl. Masel., 3, 5 (1984).

Mann, R. S., I. S. Sambi, K. C. Khulbe; Symp. on Processing Heavy Oil and Residua, Div. of Pet, Chem., ACS, Seattle Meeting, March 20-25 (1983).

Miller, J. W., M. Skripek, K. Baron, D. A. Lindsay; Proceedings of API Div. of Ref. 48th Midyear Meeting, Los Angeles, CA, May 9-12, Published by API, 62, 163 (1983).

Nielson, A., B. H. Cooper, A. C. Jacobsen; Symp. on Residua Upgrading and Coking, Div. of Pet. Chem., ACS, Atlanta Meeting, March 290April 3 (1981).

Ranganathan, R., B. B. Pruden, M. Ternan, J. M. Denis; Symp. on Refining of Synthetic Crudes, Div. of Pet. Chem., ACS, Chicago Meeting, August 28-September 2 (1977).

Sahin, R., L. Berg, F. P. McCandless; Ind. Eng. Chem. Proc. Des. Dev., 23, 495 (1984).

Sonnemans, V., F. Plantenga, P. Desai, V., D'Amico, P. Dixon; Energy Processing/Canada, May-June (1984).

Thompson, L. F., S. A. Holmes; Fuel, 64, 1, 9 (1985).

Tscheikuna, J.; M.S. Thesis, Oklahoma State University, Stillwater, Oklahoma (1984).

Wolk, R., G. Nongbri, W. Rouest; U. S. Patent No. 3,901,792, August 26 (1975).

Yeh, A. G., L. Berg, F. P. McCandless; Preprints of Div. of Fuel Chem., 23, 1, 81 (1978).

APPENDIX

DATA FROM THE ELEMENTAL ANALYSIS OF THE LIQUID PRODUCTS AND EDAX ANALYSIS OF THE CATALYST SAMPLES

Table XVII contains numerical data of the nitrogen content of the liquid products. Tables XVIII-XXVII contains data from the EDAX scans. Only metal deposits and aluminum are listed. Other support metals (Ni, Co, Mo, W, Si) are not listed.

TABLE XVII

NITROGEN CONTENT OF THE LIQUID SAMPLES

	weight percent					
time on stream (h)	CZA	CZB	CZC	CZD	CZE	CZF
6	0.158	0.159	0.494	0.468	0.648	0.218
12	0.291	0.249	0.557	0.476	0.651	0.294
18	0.352	0.267	0.593	0.494	0.662	0.339
24	0.410	0.357	0.611	0.519	0.657	0.378
30	0.476	0.402	0.640	0.582	0.701	0.384
36	0.471	0.408	0.649	0.614	0.689	0.469
42	0.538	0.464	0.679	0.629	0.733	0.507
48	0.538	0.452	0.675	0.632	0.723	0.511
60	0.538	0.470	0.687	0.657	0.767	0.509
72	0.598	*	0.692	0.682	0.779	0.525

feedstock nitrogen content 1.10 weight percent

*Sample not obtained due to early shutdown

TABLE XVIII

METAL DEPOSITION IN TOP ZONE OF RUN CZA

		area percent						
Section	Area	Al	Ca	Ti	Cr	Fe	Cu	Zn
upper	surface	47.6	3.6	7.8	-	9.3	2.8	0.7
	edge	73.2	-	-	-	1.7	2.1	0.9
	middle	74.6	-	-	-	1.5	2.1	0.8
	center	74.8	-	-	-	1.5	1.9	0.7
middle	surface	40.5	2.5	1.4	1.0	21.0	3.1	14.0
	edge	70.3	-	1.7	-	3.8	2.1	0.6
	middle	68.3	-	-	-	3.2	3.0	0.9
	center	70.7	-	-	-	2.7	2.5	-
lower	surface	50.5	1.9	2.4	1.9	16.0	2.5	0.8
	edge	52.8	1.8	5.6	-	7.1	7.1	2.5
	middle	43.2	2.3	5.2	-	6.5	5.6	1.6
	center	54.6	-	2.9	-	6.0	5.5	1.2

- Below instrument detection level

TABLE XIX

METAL DEPOSITION IN BOTTOM ZONE OF RUN CZA

		area percent						
Section	Area	Al	Ca	Ti	Cr	Fe	Cu	Zn
upper	surface	43.9	1.9	6.1	0.6	13.7	2.0	0.6
	edge	40.8	-	-	-	10.4	15.6	5.4
	middle	51.4	-	-	-	6.2	9.9	3.1
	center	45.3	-	-	-	7.5	10.8	4.1
middle	surface	43.1	3.1	11.3	-	10.2	2.8	1.0
	edge	9.1	-	-	-	1.9	31.9	13.3
	middle	67.6	-	-	-	3.2	4.8	2.1
	center	59.8	-	-	-	3.7	6.4	2.7
lower	surface	32.9	2.0	15.8	-	16.0	4.6	1.4
	edge	46.8	-	-	-	12.7	14.5	5.1
	middle	5.7	-	-	-	30.6	39.3	11.8
	center	66.4	-	-	-	5.1	5.9	2.0

- Below instrument detection level

TABLE XX

METAL DEPOSITION IN TOP ZONE OF RUN CZB

		area percent						
Section	Area	Al	Ca	Ti	Cr	Fe	Cu	Zn
—								
upper	surface	28.6	4.5	1.2	2.3	35.8	2.3	1.0
	edge	60.6	-	-	-	5.0	7.1	2.6
	middle	69.6	-	-	-	2.7	2.5	1.1
	center	43.1	3.1	11.3	-	10.2	2.8	1.0
middle	surface	34.7	5.0	3.9	1.2	17.6	5.1	1.5
	edge	2.4	-	-	-	24.6	37.0	14.3
	middle	7.6	-	-	-	25.6	35.0	12.1
	center	2.9	-	-	-	29.6	46.2	18.6
lower	surface	40.4	2.7	5.5	1.1	18.3	2.7	0.8
	edge	67.1	-	-	-	2.9	3.5	1.0
	middle	39.9	-	-	-	1.9	1.8	0.6
	center	70.2	-	-	-	2.3	2.4	0.6

- Below instrument detection level

TABLE XXI

METAL DEPOSITION IN BOTTOM ZONE OF RUN CZB

		area percent						
Section	Area	Al	Ca	Ti	Cr	Fe	Cu	Zn
upper	surface	39.5	-	5.8	-	13.3	5.5	1.6
	edge	5.6	-	-	-	19.2	28.9	10.9
	middle	17.9	-	-	-	19.5	31.6	9.7
	center	25.6	-	-	-	12.9	28.7	9.4
middle	surface	20.4	-	-	-	27.2	30.5	9.7
	edge	57.7	-	-	-	10.7	5.9	2.2
	middle	65.0	-	-	-	2.9	4.0	1.1
	center	67.5	-	-	-	2.5	3.3	0.9
lower	surface	27.6	1.4	7.6	-	17.8	19.6	10.5
	edge	62.4	-	-	-	5.2	4.5	1.6
	middle	77.8	-	-	-	1.3	1.7	0.5
	center	54.9	-	-	-	8.5	9.9	3.0

- Below instrument detection level

TABLE XXII

METAL DEPOSITION IN TOP ZONE OF RUN CZC

		area percent						
Section	Area	Al	Ca	Ti	Cr	Fe	Cu	Zn
upper	surface	33.5	2.6	1.3	1.8	28.3	3.2	1.0
	edge	12.6	-	-	-	35.6	27.0	8.7
	middle	44.5	-	-	-	12.0	9.7	3.0
	center	62.0	-	-	-	4.8	4.6	1.4
middle	surface	40.6	2.8	2.6	-	22.0	3.8	1.0
	edge	67.5	-	-	-	3.6	3.3	1.0
	middle	63.7	-	-	-	4.7	4.8	1.3
	center	57.9	-	-	-	5.9	7.1	1.9
lower	surface	28.7	1.8	2.9	1.5	33.6	3.5	1.3
	edge	56.2	-	-	-	8.9	6.6	1.9
	middle	52.5	-	-	-	7.6	9.7	2.9
	center	43.6	-	-	-	8.5	15.3	6.2

- Below instrument detection level

TABLE XXIII

METAL DEPOSITION IN BOTTOM ZONE OF RUN CZC

		area percent						
Section	Area	Al	Ca	Ti	Cr	Fe	Cu	Zn
upper	surface	4.9	2.5	4.0	-	24.6	9.6	-
	edge	6.46	-	-	-	18.2	21.5	-
	middle	29.2	-	-	-	11.2	9.4	-
	center	10.7	-	-	-	2.7	1.8	-
middle	surface	8.0	-	0.9	-	12.6	2.8	-
	edge	9.0	2.3	0.9	0.7	14.6	2.6	-
	middle	14.2	-	-	-	2.6	1.8	-
	center	10.2	-	-	-	3.3	1.9	-
lower	surface	6.6	-	-	-	28.0	13.7	-
	edge	5.3	-	-	4.1	35.6	31.6	-
	middle	7.3	-	-	-	12.6	10.7	-
	center	7.5	-	-	-	13.7	11.3	-

- Below instrument detection level

TABLE XXIV

METAL DEPOSITION IN TOP ZONE OF RUN CZD

		area percent						
Section	Area	Al	Ca	Ti	Cr	Fe	Cu	Zn
upper	surface	33.2	5.4	4.3	-	19.2	4.4	1.3
	edge	43.7	-	-	-	11.2	15.2	5.2
	middle	58.6	1.1	-	-	3.6	4.9	1.5
	center	63.7	-	-	-	3.2	3.8	1.3
middle	surface	21.9	4.0	4.7	1.5	21.7	6.9	2.7
	edge	5.9	-	-	-	34.1	32.2	8.9
	middle	8.1	-	-	-	39.1	36.5	9.0
	center	11.2	-	-	3.9	34.9	34.0	8.6
lower	surface	43.3	3.1	5.5	-	12.8	3.9	1.1
	edge	72.3	-	-	-	2.5	4.8	1.7
	middle	69.8	-	-	-	2.4	4.5	1.4
	center	72.0	-	-	-	2.3	3.4	1.1

- Below instrument detection level

TABLE XXV

METAL DEPOSITION IN BOTTOM ZONE OF RUN CZD

		area percent						
Section	Area	Al	Ca	Ti	Cr	Fe	Cu	Zn
upper	surface	31.3	2.6	8.7	-	14.0	6.4	1.9
	edge	6.7	-	-	-	31.5	34.7	9.8
	middle	64.3	-	-	-	4.3	3.9	-
	center	53.9	-	-	-	6.6	6.4	1.7
middle	surface	30.9	2.3	8.5	-	14.0	10.1	3.3
	edge	18.7	-	-	-	27.0	26.5	6.5
	middle	68.6	-	-	-	3.5	3.1	-
	center	63.8	-	-	-	4.7	4.7	1.3
lower	surface	42.1	2.6	12.6	-	8.9	2.9	1.2
	edge	68.9	-	-	-	2.9	2.7	0.6
	middle	66.9	-	-	-	3.3	2.5	0.8
	center	67.9	-	-	-	3.1	2.8	0.7

- Below instrument detection level

TABLE XXVI

METAL DEPOSITION IN TOP ZONE OF RUN CZE

		area percent						
Section	Area	Al	Ca	Ti	Cr	Fe	Cu	Zn
upper	surface	3.1	-	-	-	36.1	35.0	-
	edge	4.6	-	-	-	31.4	20.6	-
	middle	9.1	4.0	2.7	-	8.1	3.9	-
	center	10.8	2.4	1.8	-	3.1	1.4	-
middle	surface	6.5	-	-	-	7.6	2.1	-
	edge	8.9	-	-	-	4.2	2.2	-
	middle	8.8	-	-	-	4.9	2.9	-
	center	8.8	-	-	-	6.6	3.2	-
lower	surface	5.4	3.4	-	2.2	19.6	2.0	-
	edge	8.1	-	-	-	6.2	2.9	-
	middle	8.7	-	-	-	5.0	2.5	-
	center	9.0	-	-	-	5.4	3.0	-

- Below instrument detection level

TABLE XXVII

METAL DEPOSITION IN BOTTOM ZONE OF RUN CZE

		area percent						
Section	Area	Al	Ca	Ti	Cr	Fe	Cu	Zn
upper	surface	55.5	2.0	1.0	-	5.9	3.1	1.1
	edge	27.3	-	-	-	25.6	28.0	7.1
	middle	5.7	-	-	-	36.4	42.0	12.4
	center	64.1	-	-	-	4.4	4.5	1.3
middle	surface	33.6	6.7	14.0	0.8	7.7	2.5	0.9
	edge	74.0	-	-	-	1.8	2.4	0.8
	middle	59.6	-	-	-	4.7	9.2	3.3
	center	42.3	-	-	-	11.0	18.0	5.3
lower	surface	45.7	-	2.6	-	11.4	5.3	1.8
	edge	72.6	-	-	-	2.1	1.8	0.6
	middle	70.9	-	-	-	2.0	2.0	0.7
	center	69.4	-	-	-	2.3	2.4	0.8

- Below instrument detection level

VITA

ROBERT TALLEY NEWTON, JR.

Candidate for the Degree of

Master of Science

Thesis: THE EFFECT OF COMPOSITE BEDS CONTAINING CATALYSTS WITH DIFFERENT ACTIVE METALS ON THE UPGRADING OF A COAL LIQUID

Major Field: Chemical Engineering

Biographical:

Personal Data: Born in Little Rock, Arkansas, March 15, 1961. The son of Robert T. and Audrey L. Newton.

Education: Graduated from Enid High School, Enid, Oklahoma in May, 1979; received Bachelor of Science Degree in Chemical Engineering from Oklahoma State University in May, 1983; completed requirements for Masters of Science Degree in Chemical Engineering from Oklahoma State University in December, 1985.

Professional Experience: Research Assistant, School of Chemical Engineering, September, 1983 to July, 1985; Engineer Intern, Oklahoma Society of Professional Engineers; Member, National Society of Professional Engineers; Member, American Institute of Chemical Engineers.